Available online at www.sciencedirect.com
ScienceDirect
Trans. Nonferrous Met. Soc. China 26(2016) 1755−1764
Transactions of Nonferrous Metals Society of China
www.tnmsc.cn

Microstructure and dry sliding wear behavior of Cu−Sn alloy reinforced with multiwalled carbon nanotubes

H. M. MALLIKARJUNA[1,2], K. T. KASHYAP[3], P. G. KOPPAD[4], C. S. RAMESH[5], R. KESHAVAMURTHY[6]

1. Advanced Composites Research Centre (ACRC), P E S Institute of Technology, Bangalore 560085, India;
2. Department of Mechanical Engineering, GEC, K. R. Pet 571426, Karnataka, India;
3. Department of Mechanical Engineering, Atria Institute of Technology, Bangalore 560024, India;
4. Research and Development, Rapsri Engineering Products Company Ltd., Harohalli 562112, India;
5. Department of Mechanical Engineering, Alliance College of Engineering and Design, Alliance University, Bangalore 562106, India;
6. Department of Mechanical Engineering, Dayananda Sagar College of Engineering, Bangalore 560078, India

Received 26 July 2015; accepted 26 November 2015

Abstract: Multiwalled carbon nanotubes (MWCNTs) reinforced Cu−Sn alloy based nanocomposite was developed by powder metallurgy route. The mass fraction of CNTs was varied from 0 to 2% in a step of 0.5%. The developed nanocomposites were subjected to density, hardness, electrical conductivity, and friction and wear tests. The results reveal that the density of nanocomposite decreases with the increase of the mass fraction of CNTs. A significant improvement in the hardness is noticed in the nanocomposite with the addition of CNTs. The developed nanocomposites show low coefficient of friction and improved wear resistance when compared with unreinforced alloy. At an applied load of 5 N, the coefficient of friction and wear loss of 2% CNTs reinforced Cu−Sn alloy nanocomposite decrease by 72% and 68%, respectively, compared with those of Cu−Sn alloy. The wear mechanisms of worn surfaces of the composites are reported. In addition, the electrical conductivity reduces with the increase of the content of CNTs.

Key words: Cu−Sn alloy; carbon nanotube; nanocomposites; powder metallurgy; microstructure; sliding wear

1 Introduction

In last few years, nanomaterials have been extensively studied owing to their excellent performance in many engineering applications. Carbon nanotubes (CNTs) have emerged as significant materials due to their outstanding thermal conductivity of 3000 W/(m·K), mechanical strength of 63 GPa and electronic properties. On the other hand, CNTs possess certain unique characteristics, such as high elastic modulus of 2 TPa, low density, excellent lubricating behaviour and high aspect ratio, making it as an ideal reinforcement for composite materials [1−3]. Most of the conventional reinforcements have been replaced by CNTs for many engineering applications. CNTs have been tried out reinforcement in polymer, ceramic and metal matrix composites, and significant improvement in the mechanical properties has been reported [4−6].

Cu−Sn and its composites are being widely used in sliding bearings and bushes in automotive applications. In order to improve the wear characteristics, the composite materials should have a phase/reinforcement capable of providing thermal stability, strengthening and lubricating property.

In this regard, self-lubricating materials such as Cu−Sn/graphite and Cu−Sn/carbon fiber composites are promising materials with better wear resistance and lower coefficient of friction. The lubricating property of these composites is mainly due to the presence of carbonaceous materials like graphite and carbon fibers which not only reduce the friction coefficient but impart significantly the dimensional stability [7,8]. In this regard, many works have been reported on the development of Cu−Sn alloy based self-lubricating composites by adopting either powder metallurgy or casting techniques. KATO et al [9] followed powder metallurgy technique to develop Cu−Sn composites

---

Corresponding author: K. T. KASHYAP; E-mail: ktkashyap@yahoo.com
DOI: 10.1016/S1003-6326(16)64269-3

containing uncoated and copper-coated graphite and molybdenum disulfide. The developed composites showed reduction in wear rate and friction coefficient when compared with Cu−Sn alloy. Further, the Cu−Sn composites consisting of copper-coated graphite showed much lower wear rate than that of uncoated graphite. Recently, JUSZCZYK et al [10] have reported the synthesis of Cu−Sn alloy reinforced with various reinforcements like graphite, glassy carbon, WS_2 and MoS_2 by both stir casting and powder metallurgy techniques. The composites developed, especially with 20% (mass fraction) of reinforcing phase had significant resistance to wear and low friction coefficient. In addition to lubrication, the reinforcement should also possess high hardness which played an important role in deciding the wear resistance of material. In the latest developments, many researchers have focused on replacing the graphite and other lubricants with the CNTs. Compared with graphite, CNT-based metal matrix composites exhibited much higher hardness, lower friction and lower wear [11,12].

Apart from tribological studies, JUN et al [13] explored the possibility of using porous Cu−Sn composites reinforced with carbon nanotubes for oil bearing applications. The CNT reinforced porous Cu−Sn composites developed by powder metallurgy technique showed improved hardness, radical crushing strength and oil content. The oil content of 1% CNTs (mass fraction) reinforced Cu−Sn composites was 23.4% while that of Cu−Sn alloy was 20.6%. But there is limited information available on friction and wear studies on CNTs reinforced Cu−Sn composites apart from mechanical properties. The findings on tin−bronze reinforced with copper coated CNTs showed better wear resistance than that of unreinforced one and the friction coefficient decreased with increasing the volume fraction of CNTs. The decrease of coefficient of friction was attributed to the lubricating property of CNTs similar to that of graphite [14,15]. In the light of above, the present investigation dealt with microstructure, microhardness and tribological characterization of Cu−Sn nanocomposite reinforced with CNTs processed by powder metallurgy route. The mass fraction of CNT was varied from 0 to 2% in step of 0.5%. The influence of conditions (sliding velocity and load) on tribological characteristics of nanocomposites was investigated using ball-on-disc wear testing equipment.

2 Experimental

Commercial purity Cu−10Sn alloy powder and multiwalled carbon nanotubes (95% pure) with 10−30 nm in outer diameter and 1−10 μm in length were chosen as the starting materials. The mass fraction of CNTs was varied from 0.5% to 2% in a step of 0.5%. The fabrication of composites involved ball milling, compaction of composite powder, sintering and repressing. The Cu−Sn alloy powder and each mass fraction of CNTs were ball milled in a planetary ball mill (Insmart Systems, Hyderabad, India) at about 200 r/min. Maintaining a mass ratio of ball to powder of 8:1, the powders were milled for 3 h with a 10 min break intermitting every 30 min. The ball milled powders were cold- compacted in tool steel die with 20 mm in diameter for about 5 min under a pressure of 350 MPa. Then, the compacts were sintered under argon protected atmosphere at 800 °C for about 2 h. Soon after sintering, the compacts were taken out of the furnace at 800 °C and pressed under hot condition. The powder morphologies of Cu−Sn and Cu−Sn/CNT nanocomposite powders after the ball milling and the microstructures of the hot-pressed nanocomposites were studied using a scanning electron microscope (JEOL 840A JSM) and an optical microscope (Nikon Microscope LV150 with Clemex Image Analyser).

The relative densities of all the Cu−Sn and Cu−Sn/CNT nanocomposite samples were measured using Archimedes principle. The average hardness of the Cu−Sn/CNT nanocomposites was measured with the help of Shimadzu Micro Vickers hardness tester. A load of 5 N was applied for about 10 s and about 8 indentations were made at different locations on the nanocomposite samples. The electrical conductivity of all the Cu−Sn and Cu−Sn/CNT nanocomposite samples was measured using a GE AUTOSIGMA 3000 electrical conductivity meter at 20 °C. The electrical conductivity meter used the Eddy current technique for measuring the conductivity of non-ferrous metals in either Mega Siemens/meter (reciprocal ohm-meter) or %IACS (International Annealed Copper Standard). Prior to measuring the electrical conductivity, all the nanocomposites were polished. Further, the wear test was conducted on the Cu−Sn and Cu−Sn/CNT nanocomposites using a ball-on-disk type friction and wear tester (DUCOM TR20−LE). The nanocomposite samples were machined into disks with 20 mm in diameter and 5 mm in thickness. The samples were ground using emery papers to obtain a surface finish close to 0.1 μm. Hardened steel (EN 31) ball of 10 mm in diameter was used as a counterpart material. The test was performed at different loads (5, 10, 15, 20 and 25 N) at room temperature for about 30 min with ball being fixed against rotating nanocomposite sample. Before the start of each test, both the ball and nanocomposite samples were cleaned using acetone and dried. The mass losses of the alloy and nanocomposite samples after wear test were obtained. The worn surfaces of the alloy and nanocomposite disk were observed using a scanning electron microscope with EDAX attachment.

3 Results and discussion

3.1 Powder morphology

Figures 1(a) and (b) show the SEM images of as-received CNTs and Cu−Sn alloy powders, respectively. The irregularly shaped powder particles of Cu−Sn alloy are flattened due to collision between the stainless steel balls and the inside wall of vial after milling for about 3 h. The stainless steel balls which travel freely inside the vial collide with the inside wall of vial and the powder particles. Due to the impact energy imparted, the powder particles undergo significant plastic deformation and there are chances for particles to get cold welded to each other. To avoid or to reduce cold welding, ethanol is added as processing control agent which adsorbs on the powder particles surfaces and inhibits agglomerations. Figures 2(a)−(d) show the SEM images of composite powder milled for different time. Figure 2(a) shows the Cu−Sn/CNT powders milled for about 30 min in which most of CNTs protrude out of grains, while after 3 h of

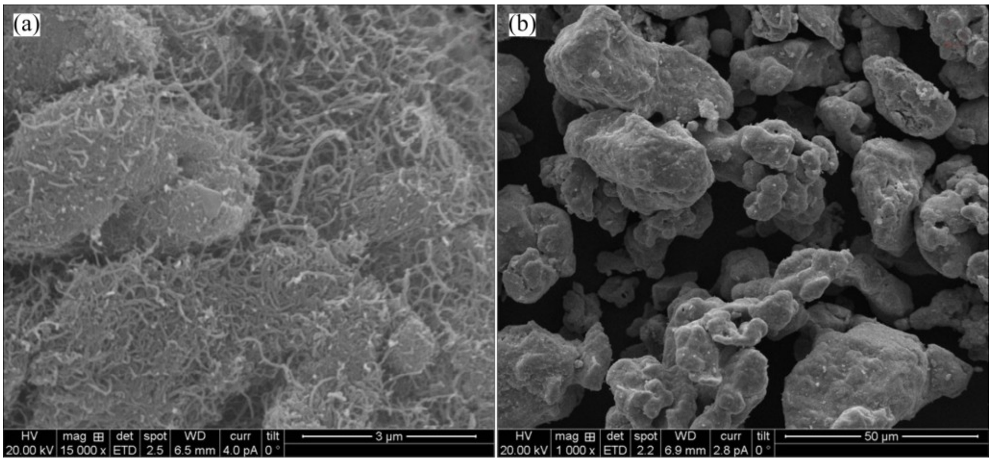

Fig. 1 SEM images of procured multiwalled carbon nanotubes (MWCNTs) (a) and Cu−10Sn alloy powders (b)

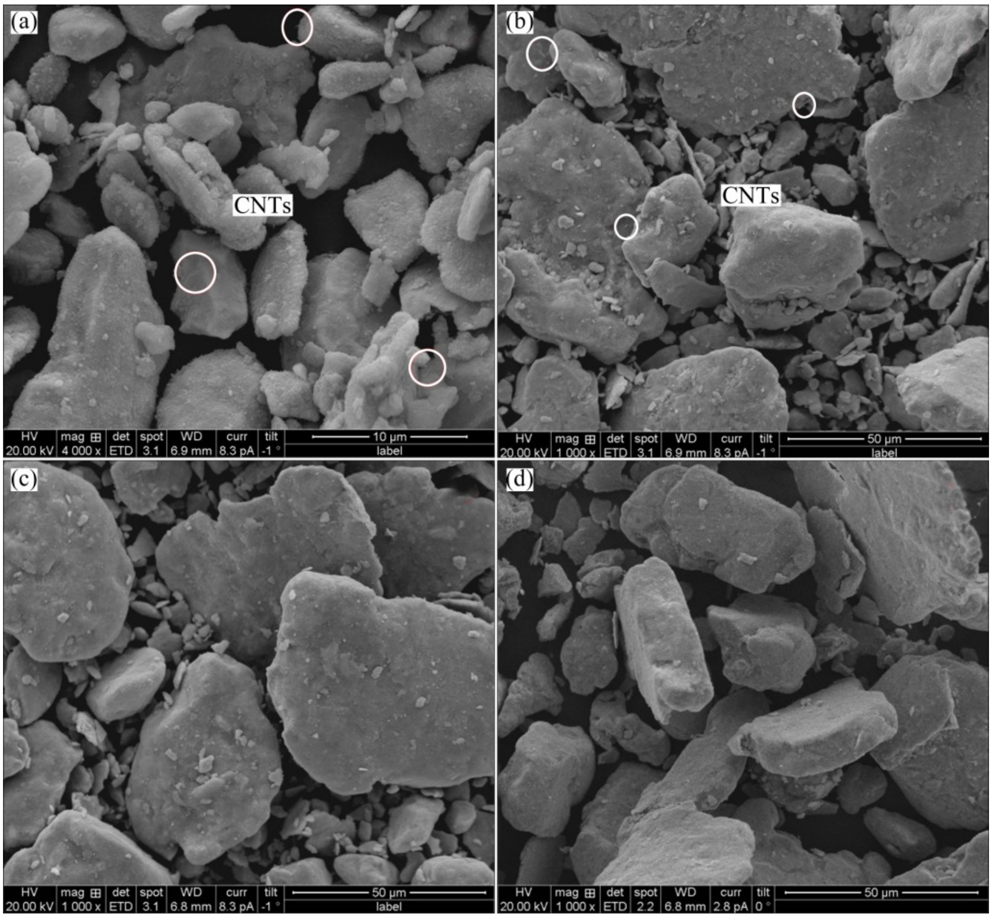

Fig. 2 SEM images of Cu−Sn/2%CNT nanocomposite powders milled for about 30 min (a), 60 min (b), 90 min (c) and 180 min (d)

milling (Fig. 2(d)), the CNTs cannot be seen on the surface of grains. The possible explanation for CNTs which cannot be observed on the surface of milled powders is that after 3 h of ball milling, the CNTs are incorporated inside and between the grains [16−18].

3.2 Relative density and microstructure

Table 1 shows the relative densities of Cu−Sn and Cu−Sn/CNT nanocomposites with various mass fractions of CNT. The technique of repressing of sintered samples was successfully employed to achieve dense nanocomposites. The relative density decreases with increasing the mass fraction of CNT due to lower density of CNTs. Figures 3(a) and (b) show the SEM images of Cu−Sn alloy and 2% CNT reinforced nanocomposites taken after hot pressing, respectively. Both the Cu−Sn alloy and nanocomposite samples show a good densification except a small number of pores in the nanocomposite, and the number of pores increases with

Table 1 Relative density of Cu−Sn and Cu−Sn/CNT nanocomposites

Composition	Theoretical density/ (g·cm^{-3})	Measured density/ (g·cm^{-3})	Relative density/%	Porosity/ %
Cu−Sn	8.78	8.72	99.32	0.68
Cu−Sn/0.5%CNT	8.64	8.56	99.07	0.93
Cu−Sn/1.0%CNT	8.51	8.36	98.24	1.76
Cu−Sn/1.5%CNT	8.38	8.18	97.61	2.39
Cu−Sn/2.0%CNT	8.25	7.92	96.00	4.00

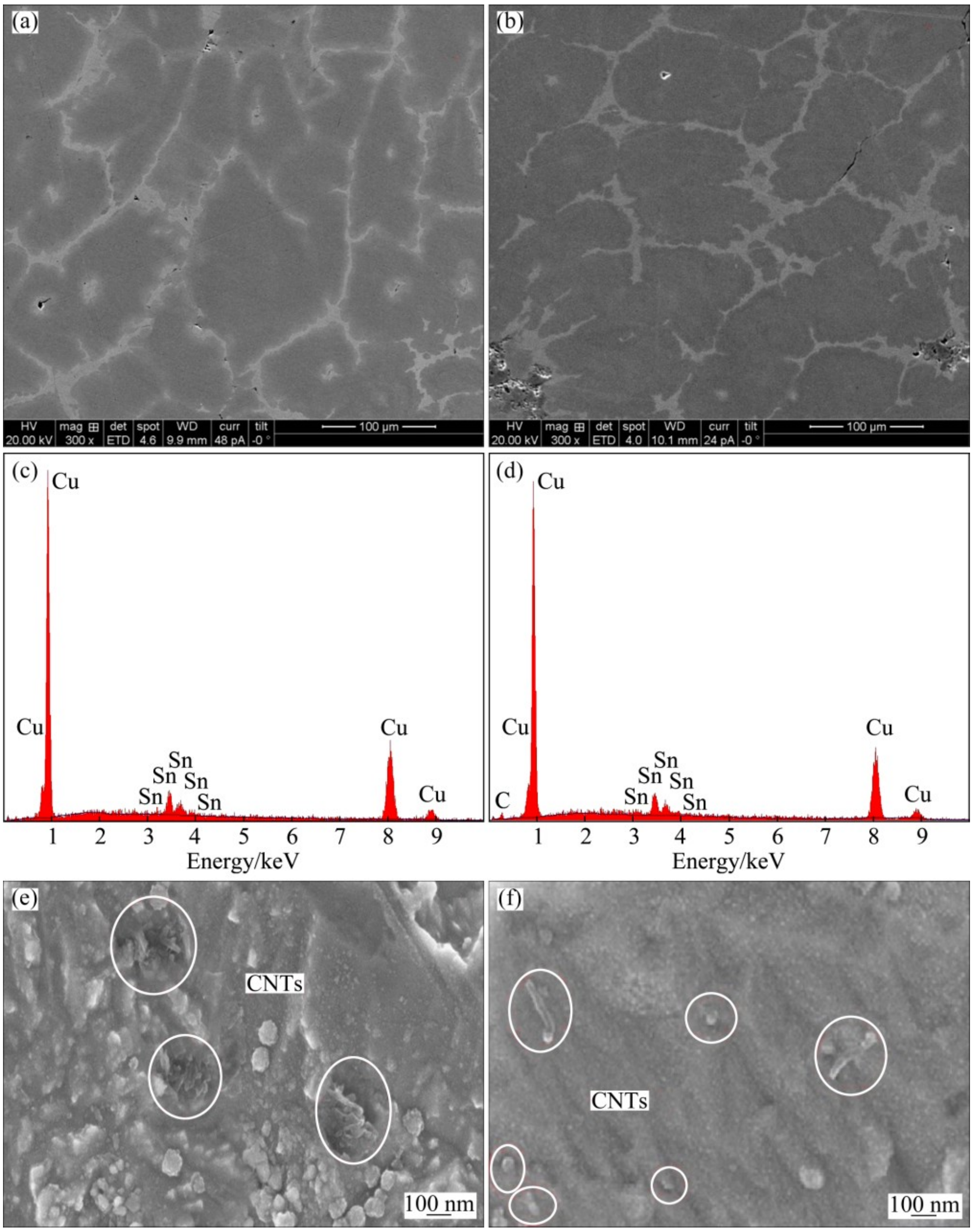

Fig. 3 SEM images (a, b) and EDS patterns (c, d) of hot-pressed Cu−Sn alloy (a, c) and Cu−Sn/2%CNT nanocomposite (b, d), and high magnification SEM images of Cu−Sn/0.5%CNT nanocomposite (e) and Cu−Sn/2%CNT nanocomposite (f)

the increase of mass fraction of CNTs. It is worth noting that the interspace between CNT and Cu−Sn grains is very minimal, indicating good interface adhesion, as shown in Figs. 3(e) and (f). The presence of Sn at the grain boundaries can be explained by the theory of equilibrium segregation which states that due to the difference in size of solute and solvent atoms, the solute atoms tend to segregate at the grain boundaries. As shown in Figs. 3(a) and (b), the tin (bright colored) is segregated at the grain boundaries. Likewise, the most of the CNTs incorporated are also seen at the grain boundaries of the matrix material. Figures 3(c) and (d) show the EDS spectra of both Cu−Sn alloy and 2% CNT reinforced nanocomposite, respectively, which explain the absence of any kinds of contamination during processing.

3.3 Hardness and electrical conductivity

Figure 4 shows the hardness of Cu−Sn/CNT nanocomposites with respect to different mass fractions of CNT. The hardness of nanocomposites shows steady increase with increasing the content of CNT. The Vickers hardness of nanocomposite with 2% CNT is HV 198, which is almost 1.17 times that of unreinforced Cu−Sn alloy. The increase of hardness is attributed to dislocations generated due to coefficient of thermal mismatch between CNTs and Cu−Sn alloy matrix. These dislocations generated at the vicinity of CNTs contribute to work hardening, leading to increased Vickers hardness. Further, CNTs act as obstacles for dislocation motion, offering large resistance to plastic deformation during hardness test, which results in improved hardness values of nanocomposites with increasing the content of CNT [19−22]. On the contrary, the nanocomposites show the decrease of electrical conductivity values with the increase of CNTs addition (Fig. 5). It is interesting to note that there is slight improvement in conductivity value of 1% CNT nanocomposite when compared with that of 0.5% CNT nanocomposite. The increase of conductivity can be attributed to straight orientation of CNTs leading to effective transportation of electrons through the CNT axis direction. Figures 3(e) and (f) show the SEM images of Cu−Sn/0.5%CNTs and Cu−Sn/1%CNTs nanocomposites, respectively. It is observed that carbon nanotubes are oriented straightly without having any kinks or damage whereas agglomeration of CNTs in few regions in 0.5% nanocomposite is found. The electrical conductivity of nanocomposites is severely affected by the MWCNTs morphology after the fabrication process. Figure 3(f) shows the straight orientation of CNTs in the Cu−Sn matrix. The improved conductivity values of 1% CNT composite can also be attributed to the ballistic transport of phonons without any interruption. Thus, the straight orientation and the absence of any kinds of agglomeration in the 1% CNT composite can be attributed to higher conductivity than that of 0.5% CNT nanocomposite [17,23,24].

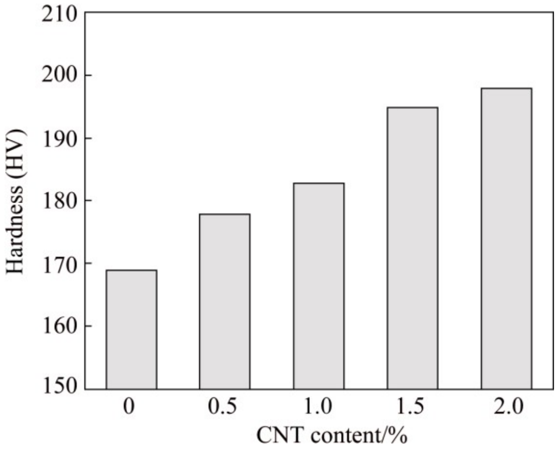

Fig. 4 Vickers hardness of hot-pressed Cu−Sn alloy and its nanocomposites with various CNT contents

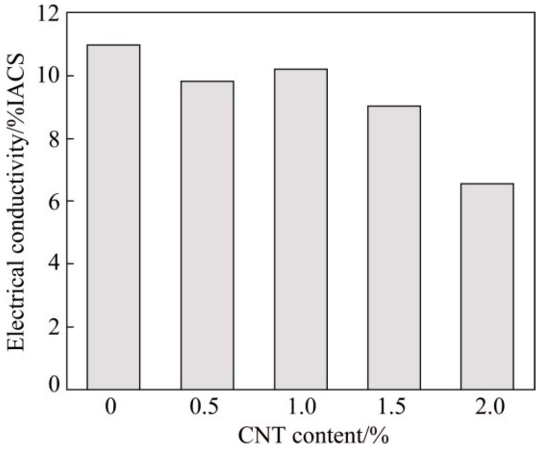

Fig. 5 Electrical conductivity of hot-pressed Cu−Sn alloy and its nanocomposites with various CNT contents

The electrical conductivity of nanocomposite with 2% CNT is 6.57% IACS in comparison with that of 11% IACS for Cu−Sn alloy. The decrease of electrical conductivity can be due to two reasons. The first reason is the presence of porosity in nanocomposites which increases with the addition of CNTs. Although the porosity fraction is not so high, they still act as insulation sites, resulting in lower conductivities. Secondly, it can be due to the scattering of electrons at the interface between CNTs and Cu−Sn matrix [17,25,26].

3.4 Coefficient of friction and wear performance

The results of coefficient of friction and wear test carried on CNT reinforced Cu−Sn nanocomposites at different mass fractions of CNT and applied loads are shown in Figs. 6 and 7, respectively. It is apparent that the content of CNTs and the load influence both the

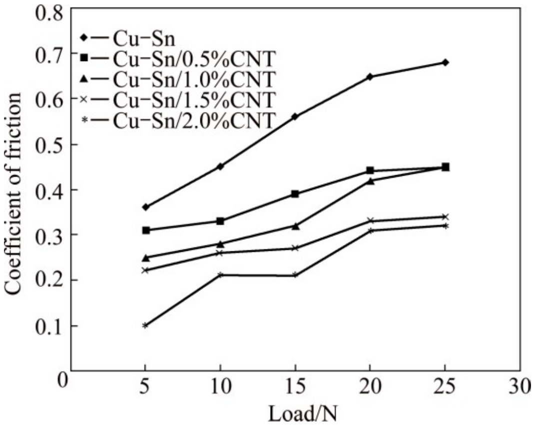

Fig. 6 Coefficients of friction of Cu−Sn/CNT nanocomposites at different mass fractions of CNT and loads (speed is 100 r/min, track radius is 16 mm, time is 30 min)

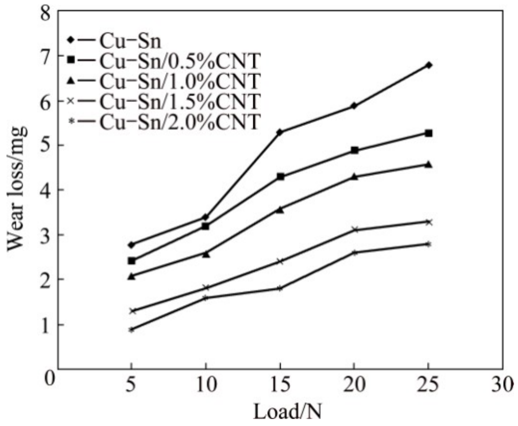

Fig. 7 Wear loss of Cu−Sn/CNT nanocomposites at different mass fractions of CNT and loads (speed is 100 r/min, track radius is 16 mm, time is 30 min)

coefficient of friction and wear characteristics of Cu−Sn/CNT nanocomposites. From Fig. 6, it can be seen that the friction coefficient of nanocomposites decreases with increasing the mass fraction of CNT. At an applied load of 20 N, the friction coefficients of unreinforced Cu−Sn alloy and 2% CNT nanocomposites are found to be 0.65 and 0.31, respectively. This shows almost 52% reduction in the friction coefficient of Cu−Sn/CNT nanocomposite compared with that of Cu−Sn alloy. The decrease of the friction coefficient can be attributed to the lubricating nature of carbon nanotubes. It is well known that the MWCNTs are composed of multiple cylindrical shells which are attached by weak van der Waals forces. During the friction process, individual shells of CNTs get worn out when they come in contact with hardened steel ball and form a thin carbon film. This carbon film formed acts as a solid lubricant between the nanocomposite disc and the hardened steel ball, leading to the decrease of friction coefficient. With increasing the mass fraction of CNT in the Cu−Sn alloy nanocomposite, it is more possible to form thicker carbon film which covers the entire wear surface, contributing to the decrease of the friction coefficient. Similar observations have been reported in bronze/CNT, Cu/CNT, and Ni−P/CNT composite systems [14,27,28].

From Fig. 7, it can be seen that the wear loss of Cu−Sn alloy is the highest. This is because of severe flaking of the alloy during sliding. As the mass fraction of CNTs goes on increasing, the wear loss decreases due to better lubrication and wear resistance provided by the CNTs at the steel ball and nanocomposite disk interface. The steady state decreasing the wear loss can be attributed to uniformly distributed CNTs in the matrix. Unlike other works [29,30] which reported the increase of wear loss with increasing the mass fraction of CNT due to poor densification and agglomeration of CNTs, the present work shows that the combination of ball milling and hot pressing is effective for processing Cu−Sn/CNT nanocomposites. In addition, the decrease of the wear loss of all nanocomposites is mainly due to the strengthening of matrix material by CNTs. However, with increasing the load from 5 to 25 N, the wear loss of Cu−Sn alloy and nanocomposites increases.

The SEM images and EDS patterns shown in Figs. 8−11 show the morphologies of worn surfaces of Cu−Sn alloy and its nanocomposites with different mass fractions of CNT. The worn surfaces of Cu−Sn alloy (Figs. 8(a) and (b)) reveal deep wear tracks and flaking debris in the worn area. The EDS analysis (Fig. 8(c)) of worn surface shows the presence of CNTs, Cu, Sn and Fe. The presence of Fe indicates the transfer of material from the hardened steel ball to Cu−Sn alloy disk due to mechanical actions during sliding, which appears to be a typical characteristic of adhesive wear. Apart from these elements, the presence of oxygen can also be seen, which explains oxidation wear mechanism along with adhesive wear [31]. In the 0.5% CNT nanocomposite, the wear mechanisms, both adhesion and oxidation, still remain the same but the extent of severity is less than that of Cu−Sn alloy. The flaking of nanocomposite with 0.5% CNT is less severe than that of Cu−Sn alloy, as shown in Figs. 9(a) and (b), and the EDS pattern of worn surface shown in Fig. 9(c).

The SEM images of worn surface of 1.5% and 2% CNT nanocomposites, as shown in Figs. 10(a) and 11(a), reveal that the wear track is smooth and free from the flaking of matrix material which is evident from the reduction in the mass losses up to 47% and 55%, respectively, compared with that of Cu−Sn alloy. Further, the analysis of worn surface of nanocomposites at higher magnification reveals that the wear mechanism changes from adhesion to abrasion. According to Fig. 9(b), the worn surfaces of 0.5% CNT nanocomposite is partially covered with lubricating carbon film. In the Cu−Sn/1.5%CNT and Cu−Sn/2%CNT nanocomposites

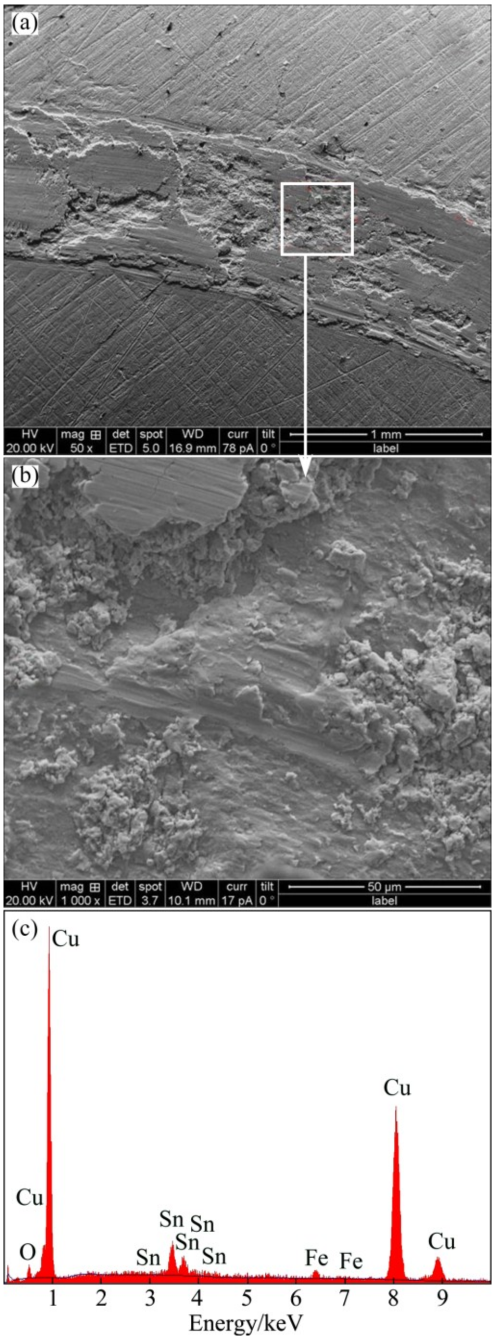

Fig. 8 SEM images (a, b) and EDS pattern (c) of worn surface of Cu−Sn alloy

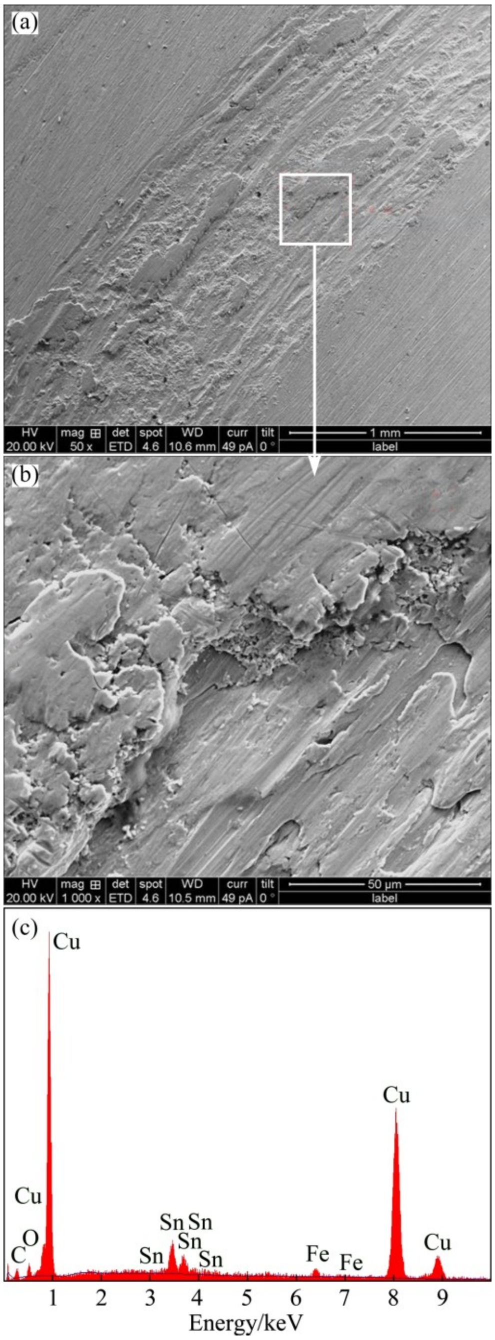

Fig. 9 SEM images (a, b) and EDS pattern (c) of worn surface of Cu−Sn/0.5%CNT nanocomposite

(Figs. 10(b) and 11(b)), the worn surface is fully covered with it. This is due to higher CNT content, and the amount of carbon film formed is significantly higher, leading to higher lubrication. The worn morphology also changes from a local flake production to a continuous distribution. This uniform dispersion of CNTs in the matrix material is very important as CNTs can effectively prevent the flaking of alloy grains. Meanwhile, the debris collected from the worn surfaces of Cu−Sn alloy and nanocomposite with 0.5% CNT are shown in Figs. 12(a) and (b), respectively. It is observed that the alloy and nanocomposite go through a severe plastic deformation, resulting in the flake like debris. These flakes form due to the formation of micro-cracks at the interface, growth of the cracks and finally peeling off from surface as the wear continues. The closer examination of wear debris shows many grinding marks on the Cu−Sn alloy flakes, whereas in the nanocomposite, the marks are less due to high hardness. Further, the small white spots on the wear debris of both alloy and nanocomposite confirm the oxidative wear mechanism along with adhesive wear mechanism. The presence of oxygen peak in the EDS pattern shown in Fig. 12(c) confirms the oxidative wear [24,32].

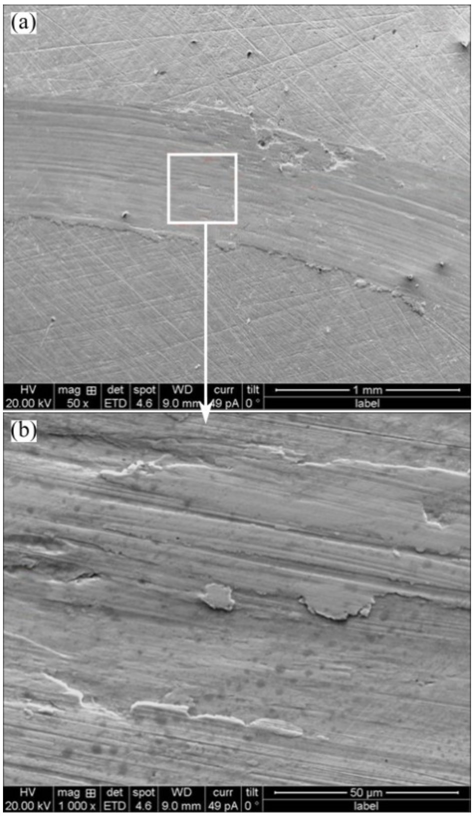

Fig. 10 SEM images of worn surface of Cu−Sn/1.5%CNT nanocomposite

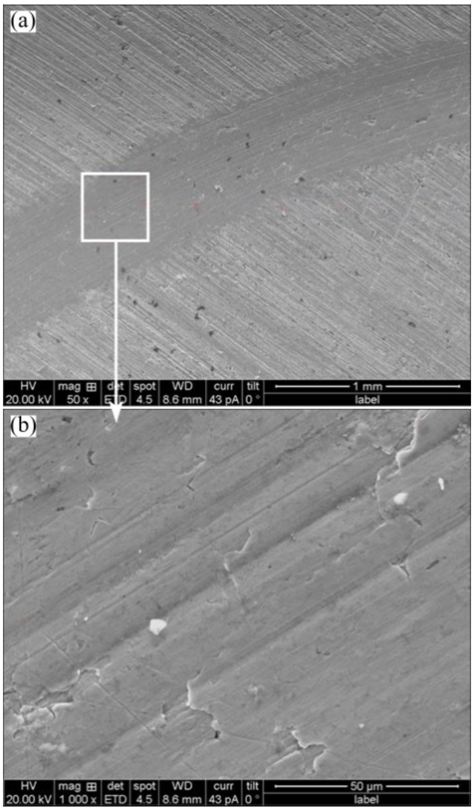

Fig. 11 SEM images of worn surface of Cu−Sn/2%CNT nanocomposite

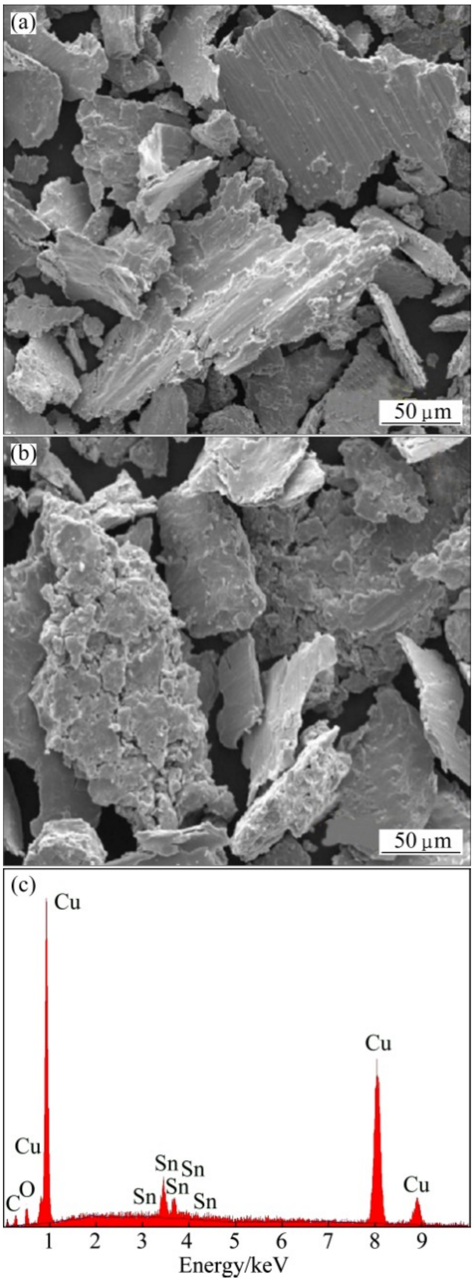

Fig. 12 SEM images of wear debris of Cu−Sn alloy (a) and Cu−Sn/0.5%CNT nanocomposite (b) and EDS pattern of Cu−Sn/0.5%CNT nanocomposite (c)

4 Conclusions

1) The nanocomposites show increased hardness with increasing the mass fraction of CNTs, but slight decrease of electrical conductivity is observed.

2) The nanocomposites exhibit lower coefficient of friction and the decrease of wear loss due to lubricating property and strengthening effect of CNTs. Cu−Sn/CNT nanocomposite with 2% CNT shows reduction in friction coefficient and wear loss by 72% and 68%, respectively, compared with that of Cu−Sn alloy when a load of 5 N was applied, but at higher load of 25 N, the reduction in

friction coefficient and wear loss are 53% and 59%, respectively.

3) The wear mechanisms operating in the Cu−Sn alloy and 0.5% CNT nanocomposite are adhesive and oxidative which later change to abrasion for nanocomposites with higher nanotubes content. On the other hand, the increase of load leads to the increase of both friction coefficient and wear loss of Cu−Sn alloy.

Acknowledgements

The authors wish to express their sincere gratitude to the following: Prof. D. JAWAHAR, CEO, PES Group of Institutions, Dr. K. N. B. MURTHY, Vice chancellor, PES University, Dr. K. S. SRIDHAR, Principal and Dr. V. KRISHNA, HOD, Department of Mechanical Engineering, PESIT, Bangalore. The critical and useful discussion of the manuscript by Dr. K. VENKATESWARLU, Materials Science Division, CSIR-National Aerospace Laboratories, Bangalore, is also acknowledged.

References

[1] RAO C N R, GOVINDARAJ A. Nanotubes and nanowires [M]. Cambridge: The Royal Society of Chemistry Publishing, 2005.

[2] POPOV V N. Carbon nanotubes: Properties and application [J]. Materials Science and Engineering R, 2004, 43: 61−102.

[3] TERRONES M. Synthesis, properties, and applications of carbon nanotubes [J]. Annual Review of Materials Research, 2003, 33: 419−501.

[4] TJONG S C. Structural and mechanical properties of polymer nanocomposites [J]. Materials Science and Engineering R, 2006, 53: 73−197.

[5] KOPPAD P G, SINGH V K, RAMESH C S, KOPPAD R G, KASHYAP K T. Advanced carbon materials and technology [M]. Hoboken: John Wiley & Sons, Inc., 2014: 331−376.

[6] PEIGNEY A, LAURENT C, FLAHAUT E, ROUSSET A. Carbon nanotubes in novel ceramic matrix nanocomposites [J]. Ceramics International, 2000, 26: 677−683.

[7] TSUYA Y, SHIMURA H, UMEDA K. A study of the properties of copper and copper-tin base self-lubricating composites [J]. Wear, 1972, 22(2): 143−162.

[8] HE D H, MANORY R. A novel electrical contact material with improved self-lubrication for railway current collectors [J]. Wear, 2001, 249(7): 626−636.

[9] KATO H, TAKAMA M, WASHIDA K, SASAKI Y, MIYASHITA S. Mechanical and wear properties of sintered Cu−Sn composites containing copper-coated solid lubricant powders [J]. Journal of the Japan Society of Powder and Powder Metallurgy, 2003, 50: 968−972.

[10] JUSZCZYK B, KULASA J, MALARA S, CZEPELAK M, MALEC W, CWOLEK B, WIERZBICKI L. Tribological properties of copper-based composites with lubricating phase particles [J]. Archives of Metallurgy and Materials, 2014, 59: 616−620.

[11] MOUSTAFA S F, EL-BADRY S A, SANAD A M, KIEBACK B. Friction and wear of copper–graphite composites made with Cu-coated and uncoated graphite powders [J]. Wear, 2002, 253: 699−710.

[12] SHUKLA A K, NAYAN N, MURTY S V S N, SHARMA S C, CHANDRAN P, BAKSHI S R, GEORGE K M. Processing of copper–carbon nanotube composites by vacuum hot pressing technique [J]. Materials Science and Engineering A, 2013, 560: 365−371.

[13] JUN L, YING L, LIXIAN L, XUEJUAN Y. Mechanical properties and oil content of CNT reinforced porous CuSn oil bearings [J]. Composites Part B: Engineering, 2012, 43: 1681−1686.

[14] ZENG J, FAN H, WANG Y, ZHANG S. Wear behavior of the lead-free tin bronze matrix composite reinforced by carbon nanotubes [J]. Metallurgical and Materials Transactions A, 2011, 42: 3858−3862.

[15] BHAT A, BALLA V K, BYSAKH S, BASU D, BOSE S, BANDYOPADHYAY A. Carbon nanotubes reinforced Cu−10Sn alloy composites: Mechanical and thermal properties [J]. Materials Science and Engineering A, 2011, 528: 6727−6732.

[16] SURYANARAYANA C. Mechanical alloying and milling [J]. Progress in Materials Science, 2001, 46: 1−184.

[17] KOPPAD P G, RAM H R A, RAMESH C S, KASHYAP K T, KOPPAD R G. On thermal and electrical properties of multiwalled carbon nanotubes/copper matrix nanocomposites [J]. Journal of Alloys and Compounds, 2013, 580: 527−532.

[18] ESAWI A, MORSI K. Dispersion of carbon nanotubes (CNTs) in aluminum powder [J]. Composites Part A: Applied Science and Manufacturing, 2007, 38: 646−650.

[19] KASHYAP K T, RAMACHANDRA C, DUTTA C, CHATTERJI B. Role of work hardening characteristics of matrix alloys in the strengthening of metal matrix composites [J]. Bulletin of Materials Science, 2000, 23: 47−49.

[20] GOH C S, WEI J, LEE L C, GUPTA M. Ductility improvement and fatigue studies in Mg−CNT nanocomposites [J]. Composites Science and Technology, 2008, 68: 1432−1439.

[21] KOPPAD P G, RAM H R A, KASHYAP K T. On shear-lag and thermal mismatch model in multiwalled carbon nanotube/copper matrix nanocomposites [J]. Journal of Alloys and Compounds, 2013, 549: 82−87.

[22] RAHUL M R, KESHAVAMURTHY R, KOPPAD P G, PRAKASH C P S. Mechanical characteristics of copper−TiB_2 composite synthesized by in-situ reaction [J]. International Journal of Applied Engineering Research, 2015, 10: 3803−3806.

[23] JIN Yu, ZHU Lin, XUE Wei-dong, LI Wen-zhen. Fabrication of super aligned carbon nanotubes reinforced copper matrix laminar composite by electro deposition [J]. Transactions of Nonferrous Metals Society of China, 2015, 25(9): 2994−3001.

[24] LI Jing-fu, ZHANG Lei, XIAO Jin-kun, ZHOU Ke-chao. Sliding wear behavior of copper-based composites reinforced with graphene nanosheets and graphite [J]. Transactions of Nonferrous Metals Society of China, 2015, 25(9): 3354−3362.

[25] KANG K, BAE G, KIM B, LEE C. Electrical and mechanical properties of multiwalled carbon nanotube reinforced Al composite coatings fabricated by high velocity oxygen fuel spraying [J]. Surface and Coatings Technology, 2012, 206: 4060−4067.

[26] LIU Z Y, XIAO B L, WANG W G, MA Z Y. Tensile strength and electrical conductivity of carbon nanotube reinforced aluminum matrix composites fabricated by powder metallurgy combined with friction stir processing [J]. Journal of Materials Science and Technology, 2014, 30: 649−655.

[27] HIPPMANN S, LI Q, ADDINAL R, VOLK W. Carbon nanotubes–reinforced copper matrix composites produced by melt stirring [J]. Journal of Nanoengineering and Nanosystems, 2013, 227: 63−66.

[28] MENG Zhen-qiang, LI Xi-bin, XIONG Yong-jun, ZHAN Jing. Preparation and tribological performances of Ni−P−multi-walled carbon nanotubes composite coatings [J]. Transactions of Nonferrous Metals Society of China, 2012, 22(11): 2719−2725.

[29] LIM D S, YOU D H, CHOI H J, LIM S H, JANG H. Effect of CNT distribution on tribological behavior of alumina–CNT composites [J]. Wear, 2005, 259: 539−544.

[30] KIM I Y, LEE J H, LEE G S, BAIK S H, KIM Y J, LEE Y Z. Friction and wear characteristics of the carbon nanotube−aluminum composites with different manufacturing conditions [J]. Wear, 2009, 267: 593−598.
[31] RAJKUMAR K, ARAVINDAN S. Tribological studies on microwave sintered copper–carbon nanotube composites [J]. Wear, 2011, 270: 613−621.
[32] GAO Yuan, JIE Jin-chuan, ZHANG Peng-chao, ZHANG Jian, WANG Tong-min, LI Ting-ju. Wear behavior of high strength and high conductivity Cu alloys under dry sliding [J]. Transactions of Nonferrous Metals Society of China, 2015, 25(7): 2293−2300.

多壁碳纳米管增强的 Cu−Sn 合金的显微组织和干滑动磨损行为

H. M. MALLIKARJUNA[1,2], K. T. KASHYAP[3],
P. G. KOPPAD[4], C. S. RAMESH[5], R. KESHAVAMURTHY[6]

1. Advanced Composites Research Centre (ACRC), P E S Institute of Technology, Bangalore 560085, India;
2. Department of Mechanical Engineering, GEC, K. R. Pet 571426, Karnataka, India;
3. Department of Mechanical Engineering, Atria Institute of Technology, Bangalore 560024, India;
4. Research and Development, Rapsri Engineering Products Company Ltd., Harohalli 562112, India;
5. Department of Mechanical Engineering, Alliance College of Engineering and Design,
Alliance University, Bangalore 562106, India;
6. Department of Mechanical Engineering, Dayananda Sagar College of Engineering, Bangalore 560078, India

摘　要：通过粉末冶金技术制备多壁碳纳米管(MWCNTs)增强的 Cu−Sn 合金纳米复合材料。CNTs 的质量分数从 0 以 0.5%的增量逐步增加到 2%，研究纳米复合材料的密度、硬度、电导率和摩擦磨损行为。结果表明：纳米复合材料的密度随 CNTs 含量的增加而降低；添加 CNTs 能显著提高纳米复合材料的硬度；相对于没有增强的合金，纳米复合材料具有低的摩擦因数和更好的耐磨性。当外加负载为 5 N 时，与 Cu−Sn 合金相比，含量为 2%的多壁碳纳米管增强的 Cu−Sn 合金纳米复合材料的摩擦因数和磨损量分别降低了 72%和 68%。报道了复合材料磨损表面的磨损机理。此外，合金的电导率随 CNTs 含量的增加而降低。

关键词：Cu−Sn 合金；碳纳米管；纳米复合材料；粉末冶金；显微组织；干滑动磨损

(Edited by Mu-lan QIN)